

# *Anthropogenic influences on heavy precipitation during the 2019 extremely wet rainy season in Southern China*

Article

Accepted Version

Li, R., Li, D., Nanding, N., Wang, X., Fan, X., Chen, Y., Tian, F., Tett, S. F.B., Dong, B. ORCID: <https://orcid.org/0000-0003-0809-7911> and Lott, F. C. (2021) Anthropogenic influences on heavy precipitation during the 2019 extremely wet rainy season in Southern China. *Bulletin of the American Meteorological Society*, 102 (1). S103-S109. ISSN 1520-0477 doi: 10.1175/BAMS-D-20-0135.1 (Li et al. (2021): Anthropogenic influences on heavy precipitation during the 2019 extremely wet rainy season in Southern China. *Bull. Amer. Meteor. Soc.*, S103-S109.) Available at <https://centaur.reading.ac.uk/95785/>

It is advisable to refer to the publisher's version if you intend to cite from the work. See [Guidance on citing](#).

To link to this article DOI: <http://dx.doi.org/10.1175/BAMS-D-20-0135.1>

Publisher: American Meteorological Society

including copyright law. Copyright and IPR is retained by the creators or other copyright holders. Terms and conditions for use of this material are defined in the [End User Agreement](#).

[www.reading.ac.uk/centaur](http://www.reading.ac.uk/centaur)

**CentAUR**

Central Archive at the University of Reading

Reading's research outputs online

# Anthropogenic influences on heavy precipitation during the 2019 extremely wet rainy season in southern China

Rouke Li<sup>1,10</sup>, Delei Li<sup>2</sup>, Nergui Nanding<sup>3,\*</sup>, Xuan Wang<sup>4</sup>, Xuewei Fan<sup>5</sup>, Yang Chen<sup>6</sup>, Fangxing Tian<sup>7</sup>, Simon F. B. Tett<sup>8</sup>, Buwen Dong<sup>7</sup>, Fraser C. Lott<sup>9</sup>

<sup>1</sup>SKLLQG, Institute of Earth Environment, Chinese Academy of Sciences, Xi'an, China

<sup>2</sup>CAS Key Laboratory of Ocean Circulation and Waves, Institute of Oceanology, Chinese Academy of Sciences, Qingdao, China

<sup>3</sup>Guangdong Province Key Laboratory for Climate Change and Natural Disaster Studies, School of Atmospheric Sciences, Sun Yat-sen University, Guangdong, China

<sup>4</sup>Key Laboratory of Mesoscale Severe Weather, School of Atmospheric Sciences, Nanjing University, Nanjing, China

<sup>5</sup> State Key Laboratory of Earth Surface Processes and Resource Ecology, Faculty of Geographical Science, Beijing Normal University, Beijing, China

<sup>6</sup>State Key Laboratory of Severe Weather, Chinese Academy of Meteorological Sciences, Beijing, China

<sup>7</sup>National Centre for Atmospheric Science, Department of Meteorology, University of Reading, Reading, United Kingdom

<sup>8</sup>School of Geosciences, University of Edinburgh, Edinburgh, United Kingdom

<sup>9</sup> Met office Hadley Centre, Exeter, United Kingdom

<sup>10</sup> National Climate Center, China Meteorological Administration, Beijing, China

\*Corresponding Author

Email: mongolnandin@gmail.com

Anthropogenic forcings have reduced the likelihood of heavy precipitation in southern China like the 2019 March-July event by about 60%

## 39 **Introduction**

40 During March to July 2019, southern China witnessed an extraordinarily long rainy season that  
41 was the 3<sup>rd</sup> wettest on record with total precipitation (1,303 mm) exceeding the climatological  
42 (1961-2010) average by 281 mm (Fig. 1a). The so-called ‘first rainy season’ (FRS), normally  
43 spanning from April to June, is the main contributor (40%-50%) to annual precipitation totals  
44 over southern China and dominates in the rainfall variability there ([Gu et al., 2018](#)). Heavy  
45 precipitation can cause flooding and landslides, resulting in huge economic losses ([Field C.B.  
46 et al., 2012](#)).

47

48 Southern China, home to the megacities like Guangzhou and Shenzhen, is highly populated,  
49 meaning a high exposure of population and infrastructure to precipitation extremes and  
50 resultant hydrological hazards ([Burke and Stott, 2017](#); [Li et al., 2018](#); [Zhang et al., 2020](#)). During  
51 6-13 June 2019, over 6 million people across several southern China provinces were affected  
52 by heavy rains, floods and landslides. These extremes caused at least 91 deaths, collapsed over  
53 19,000 houses, damaged around 83,000 houses, and affected 419,400 hectares of crops ([China  
54 Ministry of Emergency Management, 2020](#)). The direct economic loss was estimated to be  
55 more than 20 billion RMB (equivalent to 3 billion USD) ([China Ministry of Emergency  
56 Management, 2020](#)). Understanding the driver for precipitation extremes is a key step toward  
57 formulating adaptation and mitigation strategies. This study aims to shed light on this scientific  
58 question by addressing potential anthropogenic influences on the probability of extremely wet  
59 seasons similar to the March-July 2019 event in this region.

60

## 61 **Data and Methods:**

62 The March-July 2019 extreme precipitation event was bounded by 22°-28°N, 110°-120°E over  
63 southern China (Fig. 1a). Quality-controlled daily rainfall over 2,400 meteorological stations  
64 ([Shen et al., 2010](#)) during 1961-2019 were provided by the China National Meteorological  
65 Information Center. March-July 2019 precipitation at most rain-gauges in this region was  
66 around 150 mm (1mm/day) larger than normal (Fig. 1a).

67

68 Raw gauge observations were interpolated onto the 0.56° x 0.83° (same as model resolution)  
69 by using bilinear interpolation. These gridded values were area-weight averaged to obtain  
70 regional seasonal total precipitation time-series. Then precipitation time-series anomalies  
71 were calculated and the positive anomaly of 1.84 mm/day for the March-July 2019 event was  
72 used as the threshold (Fig. 1b) for the subsequent attribution analyses.

73

74 The HadGEM3-GA6 model ([Ciavarella et al., 2018](#)) at an N216 resolution of 0.56° x 0.83° was  
75 applied to investigate the role of anthropogenic forcings on the changing risks of the 2019-like

76 seasonal precipitation extremes over southern China. The model outputs include all-forced  
77 simulations (historical) conditioned on the observed sea surface temperatures (SST) and sea  
78 ice (HadISST ([Rayner et al., 2003](#))) and natural simulations (historicalNat) with anthropogenic  
79 signals removed from observed SSTs and with preindustrial forcings. Both historical and  
80 historicalNat ensembles consist of 15 members during the historical period (1961-2013), and  
81 525 members for 2019. Accordingly, occurrence probabilities and resultant attribution  
82 conclusions are conditioned on the 2019 SST patterns. The 1961-2010 climatology was  
83 constructed from the 15-member ensembles.

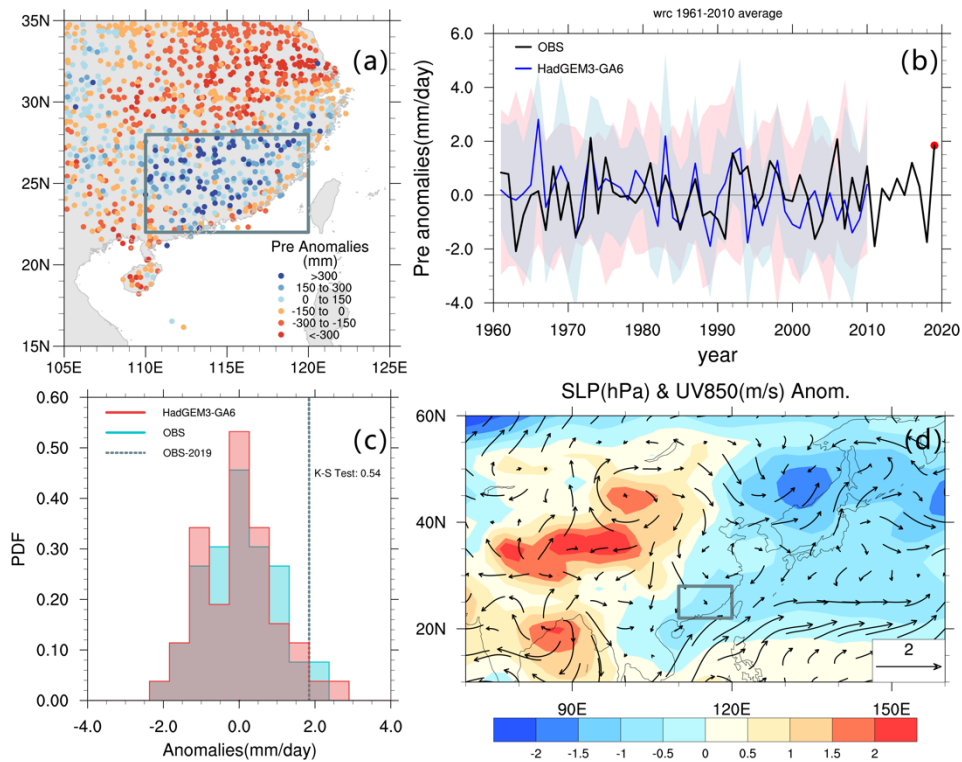
84

85 The Coupled Model Intercomparison Project Phase 5 (CMIP5) models were also included to  
86 further corroborate the attribution results. Since the historical runs terminate at the end of  
87 2005, the CMIP5 historical runs were extended through 2006 with the Representative  
88 Concentration Pathways 8.5 (RCP8.5) runs. This is because the projected greenhouse gas  
89 forcings of RCP8.5 is more consistent with the present realization than the other scenarios  
90 ([Peters et al., 2013](#)). RCP8.5 simulations for 2009–2028 are used as All and natural-only forcing  
91 runs for 1961-1980 are used as Nat (see Table. ES1 for more details). The selection of time  
92 periods for both CMIP5 All and Nat simulations is to avoid impacts from major volcano  
93 activates like 1991 eruption of Mount Pinatubo. Note that, unlike the HadGEM3-GA6  
94 simulations based on 2019 SSTs, the CMIP5 simulations encompasses a wide range of ocean  
95 states. Consequently, the event probabilities estimated hereafter are differently conditioned,  
96 such that the results from the two datasets will not be directly comparable.

97

98 A Kolmogorov–Smirnov (K-S) test was applied to test if the distributions of the observed and  
99 simulated precipitation anomalies during 1961-2010 are from the same population (Table.  
100 ES1). The occurrence probability of events with equivalent or heavier precipitation than the  
101 2019 event (anomaly of 1.84 mm/day with respect to the 1961-2010 climatology) in the entire  
102 HadGEM3-GA6 historical and historicalNat (or CMIP5 All and Nat) ensembles are indicated as  
103 PALL and PNAT respectively, and the risk ratio (RR) is computed from PALL/PNAT. The RR  
104 uncertainty with 90% confidence interval (90% CI) was estimated by identifying the empirical  
105 5<sup>th</sup> and 95<sup>th</sup> percentile amongst 1,000-times resampling of model ensemble members by using  
106 Monte Carlo bootstrapping procedure ([Christidis et al., 2013](#)). Doing each bootstrap, model  
107 ensemble simulations are randomly resampled with replacement to get a set of new data with  
108 the same length as the original. Note that precipitation anomalies estimated from each model  
109 were calculated with their own 1961-2010 climatology, serving to remove the model  
110 climatological mean bias ([Zhang et al., 2020](#)).

111



112

113 **Fig 1: (a) Observed March–July 2019 precipitation anomalies (mm/5month) from rain gauges;**  
 114 **(b) Time series of observations and simulated ensemble means of precipitation anomalies (solid lines), and uncertainty bounds of 15 members of HadGEM3-GA6 and 53 members of**  
 115 **CMIP5 spread shown as pink and blue shading, respectively. (c) Probability density functions**  
 116 **for the precipitation anomalies in the study region during March–July from 1961 to 2010**  
 117 **constructed with data from the HadGEM3-GA6 historical experiments (red) and OBS (green).**  
 118 **(d) SLP (shading) and 850-hPa wind (vector) anomalies from NCEP reanalysis in March–July**  
 119 **2019. All anomalies are relative to 1961–2010 climatology. The grey box in (a) and (d) marks**  
 120 **the study region.**

122

## 123 Results and Discussions:

124 The domain-averaged seasonal precipitation during March–July 2019 was 1.84 mm/day larger  
 125 than the 1961–2010 climatology (Fig. 1b), equivalent to a 1-in-28-yr event in the 1961–2019  
 126 observations. This prolonged extreme seasonal precipitation event was mainly due to the early  
 127 onset (by 28 days) and late cessation (by 22 days) of the first rainy season ([CMA, 2020](#)).

128

129 The event was associated with an anomalous negative sea level pressure (SLP) covering  
 130 southern China (Fig. 1d) and anomalous westerlies in the southwest of the center of the East  
 131 Asian westerly jet stream at 200-hPa (Fig. ES1d), indicating an enhanced and southward  
 132 displaced East Asian westerly jet stream in 2019. This anomalous circulation strengthens the  
 133 high-level divergence and is conducive to the enhancement of deep convection and  
 134 precipitation in southern China. The western Pacific subtropical high is enhanced and

135 extended to the southwest (Fig. ES1c). This is accompanied by 850-hPa westerly and  
136 southwesterly wind anomalies over southern China and the northeastern portion of Indochina  
137 Peninsula (Fig. 1d), which enhances the climatological mean southwesterlies in southern China  
138 (Fig. ES1f). The wind anomalies further enhance the water vapor transport from the Indochina  
139 Peninsula (Fig. ES1b). This produces anomalous moisture flux convergence over southern  
140 China (negative values in Fig. ES1e), providing a favorable moisture environment for abundant  
141 precipitation. Meanwhile, the anomalous southwesterlies advect warm air toward southern  
142 China. With more evaporation from land, increased water vapor is further enhanced. These  
143 conditions are consistent with previous studies finding that above-normal FRS precipitation is  
144 often associated with an enhanced and southwestward-extended western Pacific subtropical  
145 high and an enhanced Asian westerly jet ([Zhang et al., 2009](#); [Gu et al., 2018](#)).

146

147 Evaluation of the HadGEM3-GA6 simulations was carried out to see if this model could  
148 accurately reproduce the characteristics of precipitation in the study region. The distributions  
149 of observed and simulated precipitation anomalies (Fig. 1c) during March-July in 1961–2010  
150 cannot be distinguished based on the K-S test (P-value=0.54; Table. ES1). Note that while  
151 precipitation anomalies are reasonably simulated, the HadGEM3-GA6 overestimates actual  
152 precipitation values. Moreover, both the HadGEM3-GA6 and CMIP5 models overestimate of  
153 seasonal precipitation variability (figures omitted), leading to the underestimation of return  
154 periods for the 2019-like precipitation event, particularly for the HadGEM3-GA6 (Table. 1).  
155 These results are consistent with the precipitation variability maps shown in [Knutson and Zeng](#)  
156 ([2018](#)).

157

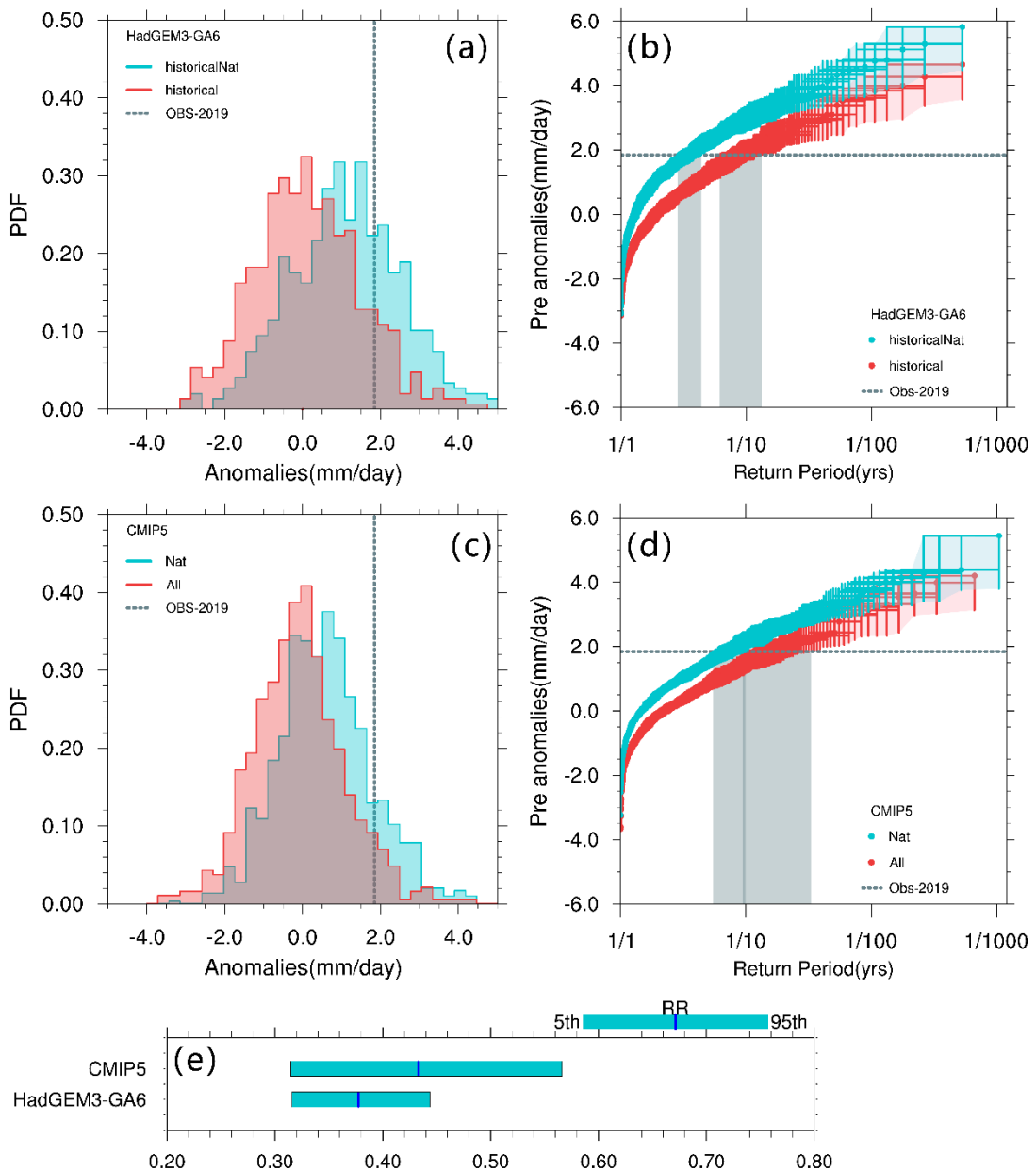
158 The probability density functions (PDFs) of the 2019-like persistent precipitation events from  
159 both models show the historical simulations shifting toward drier rainy seasons compared to  
160 the historicalNat simulations (Fig. 2a, c). This gives the estimated risk ratio of 0.43 [90% CI:  
161 0.31, 0.57] and 0.38 [90% CI: 0.32, 0.44] for CMIP5 and HadGEM3-GA6 ensembles respectively  
162 (Table. 1), which implies the anthropogenic forcings have reduced the likelihood of 2019-like  
163 extreme seasonal precipitation event over southern China by around 60%. Most of the best  
164 estimate of RR values of individual CMIP5 models are less than 1, except the GFDL-ESM2M  
165 and GISS-E2-H model (Fig. ES2). Moreover, the changes in return periods also demonstrate  
166 that the 2019-like prolonged rainy seasonal precipitation occurs less frequent due to  
167 anthropogenic influences and it changes from 1-in-4-yr event for historicalNat simulations to  
168 1-in-9-yr event for Historical simulations (Fig. 2b,d; Table. 1). Although the HadGEM3-GA6  
169 2019 simulations are atmospheric model simulations and conditional to 2019 SST pattern,  
170 their attribution results are consistent with the CMIP5 results which takes into account the  
171 variability in SST patterns.

172

173 The results are consistent with the findings in [Zhang et al. \(2020\)](#) that anthropogenic forcings

174 reduced the probability of long-lasting heavy rainfall in central western China. The reduced  
175 probability of persistent heavy rainfall due to anthropogenic forcings could be mainly due to  
176 increased aerosols in the climate system ([Song et al., 2014](#); [Li et al., 2015](#); [Zhang and Li, 2016](#);  
177 [Burke and Stott, 2017](#)). Specifically, by scattering and absorbing solar radiation, aerosols can  
178 induce surface cooling through aerosol-radiation interactions, and therefore can lead to  
179 reduced precipitation by increasing atmospheric stability. Aerosols also interact directly with  
180 cloud by serving as cloud condensation nuclei or ice nuclei, leading to changes in cloud  
181 radiative properties and reducing precipitation efficiency ([Rosenfeld et al., 2008](#)). In addition,  
182 increased aerosols can weaken land-sea thermal contrast and therefore lead to weakening of  
183 the monsoon circulation and reduced precipitation over monsoon regions ([Dong et al., 2019](#);  
184 [Zhou et al., 2020](#)). The impacts of anthropogenic forcings on changing risks of persistent  
185 precipitation events are also emphasized by the findings in [Ji et al. \(2020\)](#). They demonstrated  
186 that the anthropogenic-induced climate change has reduced the likelihood of extreme  
187 flooding by around 34% over the Yellow River basins during summer, consistent with our result.  
188 In addition, [Lu et al. \(2020\)](#) used HadGEM3-GA6 to reveal that anthropogenic forcings have  
189 reduced precipitation in favor of severe drought development during May-June over  
190 southwestern China.

191



192

193 **Fig 2: Probability density functions of (a) HadGEM3-GA6 and (c) CMIP5 All (2009-2028) and**

194 Nat (1961-1980) ensembles simulations of 2019 March-July precipitation anomalies

195 (mm/day) in the study region. Return period for the (b) HadGEM3-GA6 and (d) CMIP5 All

196 and Nat ensemble simulations. Each marker represents an ensemble member, and the green

197 and red lines are return period for the historical and historicalNat, respectively. The errors

198 bars indicate the 90% confidence interval using bootstrap resampling by 1,000 times. (e)

199 Best estimates (blue lines) and 90% confidence intervals (aqua shadings) of risk ratio for

200 CMIP5 & HadGEM3-GA6.

201

202

203

204

205

206

207 **Table 1: The best estimate and 90% confidence intervals of return period and risk ratio**  
208 **estimated with HadGEM3-GA6 and CMIP5 models.**

Models		Return Period (yrs) (90% CI)	Risk Ratio (90% CI)
HadGEM3-GA6	historical	8.78(6.12, 13.17)	0.38(0.32, 0.44)
	historicalNat	3.31(2.83, 4.35)	
CMIP5	All	15.79(9.46, 33.10)	0.43(0.31, 0.57)
	Nat	6.95(5.48, 9.92)	

209

210

211 

## Conclusions

212 Using large ensembles of HadGEM3-GA6 and CMIP5 models, anthropogenic influences on  
 213 changing risks of the 2019 March-to-July-like extreme rainy seasonal precipitation in southern  
 214 China were quantified. Results based on these two models consistently indicate similar cases  
 215 are less likely to occur in the current climate compared to the natural world. Specifically,  
 216 anthropogenic forcings have made the probability of an extreme seasonal precipitation event  
 217 like 2019 approximately 60% less likely.

218 **Acknowledgements**

219 This study was conducted during the Operational Attribution Workshop at Sun Yat-Sen  
220 University, jointly sponsored by the National Key R&D Program (2018YFC1507700), the UK-  
221 China Research & Innovation Partnership Fund through the Met Office Climate Science for  
222 Service Partnership (CSSP) China as part of the Newton Fund, and the Natural Science  
223 Foundation (NSF) of China (41975105), RL was funded by the National Key R&D Program  
224 (2017YFA0605004) and the NSF of China (41991254), DL was funded by the NSF of China  
225 (41706019) and the Strategic Priority Research Program of the Chinese Academy of Sciences  
226 (XDB42000000), NN was funded by the NSF of China (41905101) and the Fundamental  
227 Research Funds for the Central Universities (20lgpy25), ST, BD, & FL. were supported by the  
228 UK-China Research & Innovation Partnership Fund through the Met Office Climate Science for  
229 Service Partnership (CSSP) China as part of the Newton Fund.

230

231

232

233

233 **References**

234

235 Burke, C., Stott, P., 2017. Impact of anthropogenic climate change on the East Asian summer  
236 monsoon. *Journal of Climate*, 30(14): 5205-5220.

237 China Ministry of Emergency Management, 2020. 2019 Top 10 natural disasters in China,  
238 [https://www.mem.gov.cn/xw/bndt/202001/t20200116\\_343570.shtml](https://www.mem.gov.cn/xw/bndt/202001/t20200116_343570.shtml), Accessed 13  
239 April 2020

240 Christidis, N., Stott, P.A., Scaife, A.A., Arribas, A., Jones, G.S., Copsey, D., Knight, J.R., Tennant,  
241 W.J., 2013. A new HadGEM3-A-based system for attribution of weather-and climate-  
242 related extreme events. *Journal of Climate*, 26(9): 2756-2783.

243 Ciavarella, A., Christidis, N., Andrews, M., Groenendijk, M., Rostron, J., Elkington, M., Burke, C.,  
244 Lott, F.C., Stott, P.A., 2018. Upgrade of the HadGEM3-A based attribution system to  
245 high resolution and a new validation framework for probabilistic event attribution.  
246 *Weather and climate extremes*, 20: 9-32.

247 CMA, 2020. China Climate Bulletin 2019. China Meteorological Administration, 20 pp.

248 Dong, B., Wilcox, L.J., Highwood, E.J., Sutton, R.T., 2019. Impacts of recent decadal changes in  
249 Asian aerosols on the East Asian summer monsoon: roles of aerosol-radiation and  
250 aerosol-cloud interactions. *Climate Dynamics*, 53(5-6): 3235-3256.

251 Field C.B., Barros, V., Stocker, T.F., Qin, D., Dokken, D.J., Ebi, K.L., M.D. Mastrandrea, K.J.M., G.-  
252 K. Plattner, S.K. Allen, M. Tignor , (eds.), a.P.M.M., 2012. *Managing the Risks of  
253 Extreme Events and Disasters to Advance Climate Change Adaptation*. Cambridge  
254 University Press, Cambridge, UK, 582 pp.

255 Gu, W., Wang, L., Hu, Z.-Z., Hu, K., Li, Y., 2018. Interannual Variations of the First Rainy Season  
256 Precipitation over South China. *Journal of Climate*, 31: 623-640. DOI:10.1175/JCLI-D-  
257 17-0284.1

258 Ji, P., Yuan, X., Jiao, Y., Wang, C., Han, S., Shi, C., 2020. Anthropogenic Contributions to the 2018  
259 Extreme Flooding over the Upper Yellow River Basin in China. *Bulletin of the American  
260 Meteorological Society*, 101(1): S89-S94.

261 Knutson, T.R., Zeng, F., 2018. Model assessment of observed precipitation trends over land  
262 regions: Detectable human influences and possible low bias in model trends. *Journal  
263 of Climate*, 31(12): 4617-4637.

264 Li, C., Tian, Q., Yu, R., Zhou, B., Xia, J., Burke, C., Dong, B., Tett, S.F., Freychet, N., Lott, F., 2018.  
265 Attribution of extreme precipitation in the lower reaches of the Yangtze River during  
266 May 2016. *Environmental Research Letters*, 13(1): 014015.

267 Li, X., Ting, M., Li, C., Henderson, N., 2015. Mechanisms of Asian summer monsoon changes in  
268 response to anthropogenic forcing in CMIP5 models. *Journal of Climate*, 28(10): 4107-  
269 4125.

270 Lu, C., Chen, R., Jiang, J., Ullah, S., 2020. Anthropogenic influence on 2019 persistent drought  
271 in southwestern China. *Bulletin of the American Meteorological Society*, 101(1): S65-  
272 S70.

273 Peters, G.P., Andrew, R.M., Boden, T., Canadell, J.G., Ciais, P., Le Quéré, C., Marland, G.,  
274 Raupach, M.R., Wilson, C., 2013. The challenge to keep global warming below 2 °C.  
275 *Nature Climate Change*, 3(1): 4-6. DOI:10.1038/nclimate1783

276 Rayner, N.A., Parker, D.E., Horton, E.B., Folland, C.K., Alexander, L.V., Rowell, D.P., Kent, E.C.,  
277 Kaplan, A., 2003. Global analyses of sea surface temperature, sea ice, and night marine  
278 air temperature since the late nineteenth century. *Journal of Geophysical Research: Atmospheres*, 108(D14). DOI:10.1029/2002jd002670

280 Rosenfeld, D., Lohmann, U., Raga, G.B., O'Dowd, C.D., Kulmala, M., Fuzzi, S., Reissell, A.,  
281 Andreae, M.O., 2008. Flood or drought: How do aerosols affect precipitation? *science*,  
282 321(5894): 1309-1313.

283 Shen, Y., Xiong, A., Wang, Y., Xie, P., 2010. Performance of high-resolution satellite precipitation  
284 products over China. *Journal of Geophysical Research: Atmospheres*, 115(D2).  
285 DOI:10.1029/2009jd012097

286 Song, F., Zhou, T., Qian, Y., 2014. Responses of East Asian summer monsoon to natural and  
287 anthropogenic forcings in the 17 latest CMIP5 models. *Geophysical Research Letters*,  
288 41(2): 596-603. DOI:10.1002/2013gl058705

289 Zhang, J., Zhou, T., Yu, R., Xin, X., 2009. Atmospheric water vapor transport and corresponding  
290 typical anomalous spring rainfall patterns in China. *Chin. J. Atmos. Sci.*, 33(1): 121-134.

291 Zhang, L., Li, T., 2016. Relative roles of anthropogenic aerosols and greenhouse gases in land  
292 and oceanic monsoon changes during past 156 years in CMIP5 models. *Geophysical  
293 Research Letters*, 43(10): 5295-5301. DOI:10.1002/2016gl069282

294 Zhang, W., Li, W., Zhu, L., Ma, Y., Yang, L., Lott, F.C., Li, C., Dong, S., Tett, S.F., Dong, B., 2020.  
295 Anthropogenic Influence on 2018 Summer Persistent Heavy Rainfall in Central  
296 Western China. *Bulletin of the American Meteorological Society*, 101(1): S65-S70.

297 Zhou, T., Zhang, W., Zhang, L., Zhang, X., Qian, Y., Peng, D., Ma, S., Dong, B., 2020. The dynamic  
298 and thermodynamic processes dominating the reduction of global land monsoon  
299 precipitation driven by anthropogenic aerosols emission. *Science China Earth Sciences*,  
300 63(7): 919-933.

301